American Journal of Ophthalmology Case Reports 32 (2023) 101873

Contents lists available at ScienceDirect

American Journal of Ophthalmology Case Reports

journal homepage: www.ajocasereports.com/

Durable vision improvement after a single intravitreal treatment with antisense oligonucleotide in *CEP290*-LCA: Replication in two eyes

Artur V. Cideciyan [a,*], Samuel G. Jacobson [a,1], Allen C. Ho [b], Malgorzata Swider [a], Alexander Sumaroka [a], Alejandro J. Roman [a], Vivian Wu [a], Robert C. Russell [a], Iryna Viarbitskaya [a], Alexandra V. Garafalo [a], Michael R. Schwartz [c], Aniz Girach [c]

[a] *Scheie Eye Institute, Department of Ophthalmology, Perelman School of Medicine, University of Pennsylvania, Philadelphia, PA, USA*
[b] *Wills Eye Hospital, Thomas Jefferson University, Philadelphia, USA*
[c] *ProQR Therapeutics, Leiden, the Netherlands*

ARTICLE INFO

Keywords:
Cone photoreceptors
Intravitreal injection
LCA10
Leber congenital amaurosis
NPHP6
QR-110
Retinal degeneration

ABSTRACT

Purpose: An intravitreally injected antisense oligonucleotide, sepofarsen, was designed to modulate splicing within retinas of patients with severe vision loss due to deep intronic c.2991 + 1655A > G variant in the *CEP290* gene. A previous report showed vision improvements following a single injection in one eye with unexpected durability lasting at least 15 months. The current study evaluated durability of efficacy beyond 15 months in the previously treated left eye. In addition, peak efficacy and durability were evaluated in the treatment-naive right eye, and re-injection of the left eye 4 years after the first injection.

Observations: Visual function was evaluated with best corrected standard and low-luminance visual acuities, microperimetry, dark-adapted chromatic perimetry, and full-field sensitivity testing. Retinal structure was evaluated with OCT imaging. At the fovea, all visual function measures and IS/OS intensity of the OCT showed transient improvements peaking at 3–6 months, remaining better than baseline at ~2 years, and returning to baseline by 3–4 years after each single injection.

Conclusions and Importance: These results suggest that sepofarsen reinjection intervals may need to be longer than 2 years.

1. Introduction

Inherited retinal diseases (IRDs) make up a heterogeneous group of conditions in which thousands of distinct disease causing variants in more than 300 different genes act on rod or cone photoreceptors to cause vision loss that can range from barely noticeable to complete blindness.[1,2] Natural histories of IRDs often vary in terms of disease onset, location and type of retinal cells involved, and spread and rate of progression. Main phenotype of each IRD can be either degeneration-only, where vision loss is proportionate to photoreceptor loss, or dysfunction-only, where there is abnormal visual function despite structurally retained photoreceptors, or there is a combination of degeneration and dysfunction. Depending on the main phenotype, the aim of treatments for IRDs is to prevent photoreceptor degeneration, or ameliorate dysfunction, or both. Despite the enormous effort spent over the last 15 years, it has been possible to deliver an approved treatment for only one IRD to date.[3]

The most severe forms of IRDs, both non-syndromic forms as well as retinal manifestations of syndromic forms, typically are associated with the diagnosis of Leber congenital amaurosis (LCA). There are more than 20 molecular causes of LCA[4] and approximately one third of them are retina ciliopathies caused by genes that are expressed at the connecting cilium of rod and cone photoreceptors. One of the most common forms of LCA is also a retinal ciliopathy caused by *CEP290* variants.[5,6] The phenotype of *CEP290*-LCA is complex but well studied.[7–15] Patients typically show a severe degeneration of rod photoreceptors that tends to sweep across the retina within the first decade of life. Central cone photoreceptors are retained for many decades but often show dysfunction. The most common allele in *CEP290*-LCA is c.2991 + 1655A > G p.(Cys998*) which is thought to cause aberrant splicing in some

* Corresponding author.
E-mail address: artur.cideciyan@pennmedicine.upenn.edu (A.V. Cideciyan).
[1] Deceased.

https://doi.org/10.1016/j.ajoc.2023.101873
Received 28 March 2023; Received in revised form 15 May 2023; Accepted 11 June 2023
Available online 20 June 2023

mRNA transcripts and introduction of a cryptic exon containing a premature stop codon. A therapeutic strategy involving antisense oligonucleotides (AONs) preventing the insertion of the mutant CEP290 pseudo-exon into the mRNA was hypothesized[16,17] and a clinical drug candidate – QR110 or sepofarsen - was produced.[18]

Eleven individuals with *CEP290*-LCA due to at least one c.2991 + 1655A > G allele participated in the phase 1b/2 trial of intravitreal sepofarsen between late 2017 and late 2019 (NCT03140969; EudraCT 2017-000813-22). Safety and efficacy results from this trial are published.[19–22] The initial Phase 1b/2 trial was extended to evaluate contralateral eye injections as well as continued injections in the first treated eyes beyond 12 months (NCT03913130; EudraCT 2018-003500-40) and nine of the eleven individuals chose to participate. Current work provides results from a hyper-responder patient P11 who participated in both the initial trial and the extension.

2. Methods

Study medication and trial design. This study complies with all relevant ethical regulations and was approved by the institutional review board of the University of Pennsylvania. The study was conducted according to the Declaration of Helsinki as well as according to the principles of Good Clinical Practice. Eleven individuals with *CEP290*-LCA participated in the initial phase 1b/2 trial of sepofarsen (NCT03140969, EudraCT 2017-000813-22), and a subset of nine individuals participated in a follow-on extension trial (NCT03913130; EudraCT 2018-003500-40). All participants had biallelic variants in *CEP290*, at least one of which was the common c.2991 + 1655A > G allele. Some of the results from the trial have been previously published.[19–22] A phase 3 trial (NCT03913143, EudraCT 2018-003501-25) was also performed but no results have been published to date.

Sepofarsen (aka. QR-110) is a 17-mer single-stranded 2′-O-methyl modified phosphorothioate RNA antisense oligonucleotide (AON) designed for potential treatment of the vision loss experienced by subjects with Leber congenital amaurosis (LCA) due to the CEP290 c.2991 + 1655A > G variant.[18] Sepofarsen is thought to bind to the exonic splicing enhancer sequence at intron 26 of the CEP290 pre-mRNA and modulate the RNA splicing process, blocking access to the active cryptic splicing site, and restoring preference for the wildtype splicing sites. A resulting increase of wildtype mRNA transcript is predicted to lead to an increase of functional CEP290 protein.

An open-label study was designed to evaluate the safety and tolerability of sepofarsen administered via unilateral intravitreal (IVT) injection every three months for up to 1 year followed by an extension study where the first treated and contralateral eyes would be injected three months apart with each eye being dosed no more frequently than once every 6 months. The same dose level would be used for both eyes in the extension study. Dose level and/or dose interval could be modified considering safety and/or efficacy signals.

Safety evaluations. Ocular safety was assessed with standard eye examinations, including gradings of the anterior and posterior segment, and of the lens. Systemic safety was evaluated with a complete physical examination at screening and symptom-directed physical exams at subsequent visits, electrocardiograms performed pre-dose, and vital sign measurements taken at all study visits. Routine hematology, serum chemistry, and INR measures were performed at screening and pre-dosing visits through M3 of the extension study. For P11, regarding general and systemic parameters, there were no clinically significant changes in hepatic and renal functions, assessed by liver enzymes and glomerular filtration rate, respectively. There was no intra-ocular inflammation and no cystoid macular edema noted throughout the 48-month observation period. In the left eye, at 30 months after the first injection, there was a transient appearance of a small posterior subcapsular cataract but it had spontaneously resolved by the next visit at 34 months. There were no lenticular changes noted in the right eye throughout the 48-month observation period.

Outcome measures of visual function and retinal structure. Measures of visual function and imaging of the retinal and RPE microstructure were performed per clinical trial protocol. Importantly, all pretreatment measures were duplicated at two visits ~30 days apart. In addition, P11 was a patient of our center for hereditary retinal degenerations and was evaluated two years previous to the enrollment with detailed non-invasive assessments of visual function and retinal structure (P8 in Ref. 11). Contemporaneous with the clinical trial, P11 was enrolled in additional research studies that had been approved by the University of Pennsylvania Institutional Review Board. These specialized non-invasive assessments provided further details of visual function and retinal structure that expanded the findings from the clinical trial protocol.

Visual acuity. Best corrected visual acuity (BCVA) was measured using Early Treatment Diabetic Retinopathy Study (ETDRS) methodology.[23] LLVA was measured with a 2ND filter in a darkened room[24,25] starting at month 3 following first injection in the left eye continuing through the end of the study.

Full-field Stimulus Testing (FST). Sensitivity to light flashes with full-field stimulus testing (FST) was developed specifically for patients with severe vision loss and oculomotor instability.[26–29] FSTs were performed with red, blue and white stimuli under dark-adapted and light-adapted conditions using a single button 4/2 dB staircase with two response reversals and a limited response-acceptance window to minimize the effect of extraneous responses not synchronized with the stimulus presentation. At all visits, in both eyes, under dark-adapted and light-adapted conditions, the differences between red and blue thresholds were consistent with mediation by cones. Therefore, average of red, blue and white thresholds is presented.

Perimetry. Dark-adapted free-viewing static perimetry (Humphrey Field Analyzer, HFA-750i analyzer, Zeiss-Humphrey, Dublin, CA, USA) with monochromatic red (650 nm) and blue (500 nm) stimuli (Goldmann V, 200 ms) was performed along the horizontal and vertical meridian.[29] A single red fixation was used to obtain sensitivities at locations surrounding the fovea, and four red lights forming a small diamond were used to obtain sensitivity of the fovea. At all visits, in both eyes, the differences between red and blue thresholds were consistent with mediation by cones. Therefore, average of red and blue thresholds is presented. A retina-tracking microperimeter (MP1, Nidek Inc, Fremont, CA) was used with white stimuli (max luminance = 127 cd m^{-2}, Goldmann V, 200 ms) presented on a red background (1 cd m^{-2}). Thresholds were collected with two different patterns: along a horizontal profile oversampled at 0.5° intervals, and a two-dimensional "macula 8" pattern with sampling intervals ranging from 0.5° to 1.4°. A criterion sensitivity of 3 dB was used to estimate the extent of the visual field.

Mobility. Functional vision was evaluated under dark-adapted conditions as described previously.[25,30] In brief, vertical LED strips on a plane resembling a beaded curtain were programmed to produce a rectangular pattern target defining a 'door' of varying luminance that could appear at one of three positions. The subject began the task at a starting position ~4 m away from the device and was instructed to proceed to touch the door. Success was defined as the subject touching within the 'door' area. The test was performed monocularly in the dark-adapted state and with dilated pupils. The dimmest scene luminance used was near the absolute functional vision threshold for normal scotopic vision. Mobility performance at different scene illuminations was evaluated using percent success of navigation over a fixed number of trials. The success/not success data at each set (10 trials) of all luminance steps tested were fit individually for each eye by logistic regression with asymptotes of 0.3 and 1.0. The threshold for successful travel was defined as the luminance corresponding to 65% success on the fitted curve.

En face retinal imaging. Near-infrared autofluorescence (NIRAF) imaging was performed per clinical trial protocol using a confocal scanning laser ophthalmoscope (Spectralis HRA, Heidelberg Engineering, Heidelberg, Germany) as previously described.[7,8,29,31] For each eye,

NIRAF images from all visits were spatially aligned to the first baseline image (MATLAB, Mathworks, Natick, MA). Across all aligned images, NIRAF signal intensity profile was calculated along 0.58°-wide bands centered on the fovea along the horizontal and vertical meridians. Each profile was normalized by the average autofluorescence intensity within ±3° eccentricity of the fovea to compare the extents of centrally retained elliptical regions over the follow up visits to baseline. The extents were quantified by the locus of intersection between two lines fit to portions of the NIRAF profiles. All extent data are plotted as change from eye-specific baseline (Table S1).

Cross-sectional retinal imaging. Spectral-domain Optical Coherence Tomography (OCT) was used to obtain cross-sectional imaging of the retina (RTVue-100; Optovue, Fremont, CA) per clinical trial protocol. All OCT images were aligned by straightening the major RPE reflection. Quantitative analyses of the retinal sub-lamination thicknesses and the backscatter intensity of the peak originating near the junction of inner and outer segments was performed using longitudinal reflectivity profiles (LRP).[8,29,32] In brief, groups of 34 neighboring LRPs were averaged at 5 locations centered at the foveal center, 1° and 2° eccentricity on horizontal scans. Peaks corresponding to retina-vitreous interface (RVI), outer plexiform layer (OPL), external limiting membrane (ELM), IS/OS junction, and OS/RPE junction were manually defined on three independent sets of data obtained in each eye at each visit. Layer thicknesses of total retina (RVI to OS/RPE), ONL (OPL to ELM), IS (ELM to IS/OS), OS (IS/OS to OS/RPE) were calculated. Normalized IS/OS reflectivity was estimated as the difference of IS/OS peak backscatter value at each sampled location from the average ILM backscatter value obtained across all sampled locations from a 15 μm slab choroidal to the RVI. All thickness and reflectivity data are plotted as change from eye-specific baseline (Table S2).

3. Results

When first enrolled into the phase 1b/2 study, patient 11 (P11) was 14 years old; for the next 4 years, visual function and retinal structure were periodically evaluated (Fig. 1A, black circles) as intravitreal injections of 160 μg sepofarsen were delivered (Fig. 1A, red stars). First left eye was dosed, 15 months later the right eye was dosed, and the left was re-dosed 2.75 years after the right eye injection and 4 years after the first left eye injection. Some results obtained for the first 15 months following the first left eye injection have been previously published[20] but results between 15 months and 4.25 years after enrollment are novel (Fig. 1A).

At enrollment, P11 had central elliptical islands of retained retinal pigment epithelium (RPE) melanization readily apparent on NIRAF imaging and retained region of photoreceptors with inner and outer segment (IS/OS) signal detectable on optical coherence tomography (OCT, Fig. 1B). Boundaries of the central islands of structural retention were symmetric across both eyes (Fig. 1B, inset).

At baseline, best corrected visual acuities (BCVA) were symmetric at 53 letters (0.64 logMAR or Snellen equivalent 20/80). In the left eye, as reported previously,[20] between 5 and 7 months after a single sepofarsen injection, BCVA had improved by 10–13 letters (representing ~2 lines on the chart). Over the next 4 years, there was a tendency for the visual acuity to slowly return towards baseline (Fig. 2A, white symbols). At four years following the first injection, left eye was reinjected and showed a 7 letter improvement at three months (Fig. 2A, gray symbol). Initially uninjected right eye was followed for 15 months during which the average BCVA was 57.3 letters (Fig. 2A gray horizontal line) with a tendency for slight improvement over time. The visit at three months after the right eye injection was missed due to the pandemic. At six months after the first injection in the right eye, BCVA had improved by 7 letters. Over the next 3 years, there was a tendency for a slow return towards baseline (Fig. 2A, black symbols).

Since sepofarsen is not expected to increase the number or density of

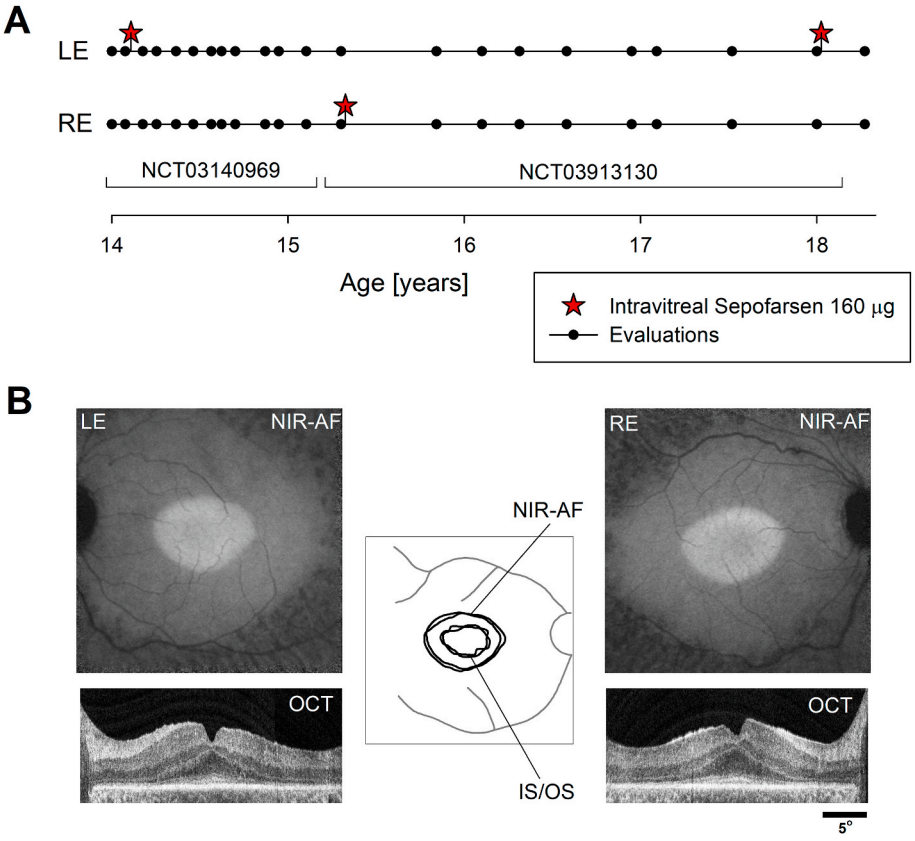

Fig. 1. Study overview and symmetry at baseline. **(A)** Schematic overview of the 4+ yearlong study started with the enrollment of the subject P11 at age 14. Timing of the intravitreal injections are shown with respect to the visual function and retinal imaging evaluations performed during the initial (NCT03140969) and the extension (NCT03913130) segments of the phase 1b/2 clinical trial. Some of the results from the first 15 months have been previously published. **(B)** En face NIRAF images and cross-sectional OCT images of both eyes at baseline. Outlines of the NIRAF melanization and OCT IS/OS boundaries (inset center) show close interocular symmetry of retinal structure.

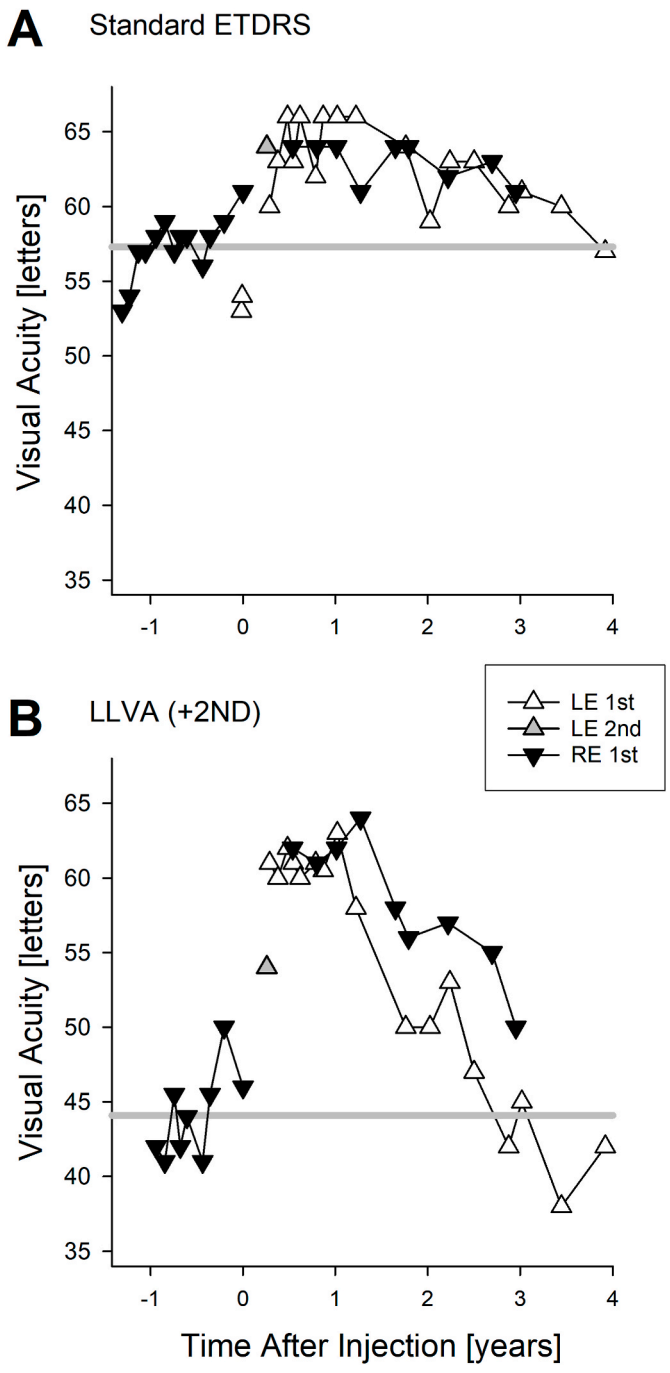

Fig. 2. Standard ETDRS best corrected visual acuity (**A**) and low-luminance visual acuity (LLVA) with a 2 ND filter (**B**) in each eye (RE, black down triangles; LE, white or gray up triangles) as a function of time from each sepofarsen injection. Visual acuity specified as number of letters read correctly at 4 m distance plus 30. Average acuities in the RE during the 15 month pre-injection period (horizontal gray lines) were 57.3 letters (0.55 logMAR or 20/80 Snellen equivalent) for standard ETDRS and 44.1 letters (0.82 logMAR or 20/125 Snellen equivalent) for LLVA, respectively.

photoreceptors, we hypothesized that any potential changes to BCVA would likely originate from changes in light sensitivity of photoreceptors. Measured acuity reduces when illumination reaching the photoreceptors is reduced either by intercalated neutral density filters[33] or by disease-induced loss of foveal sensitivity.[34] To evaluate the relation between acuity and retinal illuminance in treated and untreated eyes of P11, we performed low-luminance visual acuity (LLVA) measurements with a 2 log unit neutral density filter reducing the luminance of the ETDRS chart in a darkened room starting at 3 months after first injection in the left eye. LLVA in the treated left eye was comparable to standard ETDRS BCVA between 3 and 12 months (Fig. 2A and B, white symbols). Thereafter, LLVA in the left eye reduced progressively over the next 3 years. Upon re-injection of the left eye, LLVA improved by 12 letters (Fig. 2B, gray symbol). Average LLVA in the initially uninjected right eye over 11 months was 44.1 letters (Fig. 2B gray horizontal line). After a single injection, LLVA improved by 18–20 letters (3–4 lines) between 6 and 15 months (Fig. 2B, black symbols). There was a progressive reduction of LLVA thereafter. At three years post-injection, LLVA was within 0–9 letters of baseline. Standard BCVA and LLVA results can be interpreted as a combination of learning/motivation driven and potentially sepofarsen-driven improvement. Learning/motivation appears to contribute to variability of up to 8–9 letters to both forms of acuity. Sepofarsen-driven changes appear to peak between 3 and 6 months post injection with 3–11 letter improvement for ETDRS and 14–23 letter improvement for LLVA. Low-luminance deficit was reduced from 15.1 letters on average pre-treatment to 3.9 letters on average post-treatment. The latter value was similar to that reported in normal eyes.[35]

Sensitivity to light was directly measured with several psychophysical methods, and different color stimuli and ambient conditions. We used white stimuli presented on a red background with retina-tracking perimetry to compensate for the fine nystagmus (Fig. 3A). Test locations were divided into regions representing foveal center (up to 1.4° eccentric), foveal edge (1.5–2.5° eccentric) and the parafovea (2.5-4° eccentric). After the first injection in the left eye, there was an improvement of 17 dB at the foveal center, and 10 dB at the foveal edge; improvements in the parafovea were mostly non-detectable (Fig. 3A, white symbols). Starting after 1 year, both foveal center and edge locations showed slow progressive reduction of sensitivities asymptoting towards baseline over the next three years. Three months after the second injection in the left eye, there was a similar improvement pattern as after the first injection (Fig. 3A, gray symbols).

To better understand absolute light sensitivity of P11's photoreceptors, we used blue and red stimuli under dark-adapted conditions with free-viewing perimetry. At all locations, at all visits, blue-red differences were consistent with cone mediation. Therefore, we averaged blue and red sensitivities. At the center of a diamond shaped fixation pattern (corresponding closely to the center of anatomical fovea), dark-adapted sensitivity at baseline was near −0.8 log phot-cd.m^{-2} in both eyes. Between 3 and 12 months after the first injection in the left eye, there was a 0.5 log improvement with a slow trend of reduction towards baseline thereafter (Fig. 3B, white symbols). At 6 months after the first injection in the right eye, there was a 1 log improvement followed by trend towards baseline (Fig. 3B, black symbols). At 3 months after the second injection in the left eye, the improvement was 1 log (Fig. 3B, gray symbol). At the foveal edge, baseline sensitivities were worse than foveal center, but the improvement following first and second injections were larger than 1 log. At the parafovea, there was no substantial change detectable over time.

Since sepofarsen is provided as an intravitreal injection, it has the potential to change the function of any photoreceptors remaining across the whole retina. To evaluate such potential changes beyond the central retina, we used full-field sensitivity testing (FST) with blue, red and white stimuli presented homogeneously across the visual field. Both dark-adapted and light-adapted conditions were used. Under all conditions across all visits in both eyes, sensitivities to three spectral colors were consistent with cone mediation. Therefore, we averaged blue, red and white sensitivities. At baseline, dark-adapted FST sensitivity was −1.3 and −1.1 log phot-cd.m^{-2} in right and left eyes, respectively. By 3–6 months following all injections, there was an improvement of 0.8–0.9 log units followed by steady slow decline that reached baseline between 3 and 4 years post-injection (Fig. 3C). At baseline, light-adapted FST sensitivity was −0.1 and −0.4 log phot-cd.m^{-2} in right and left eyes, respectively. Post-injection improvement was smaller ranging 0.3–0.4

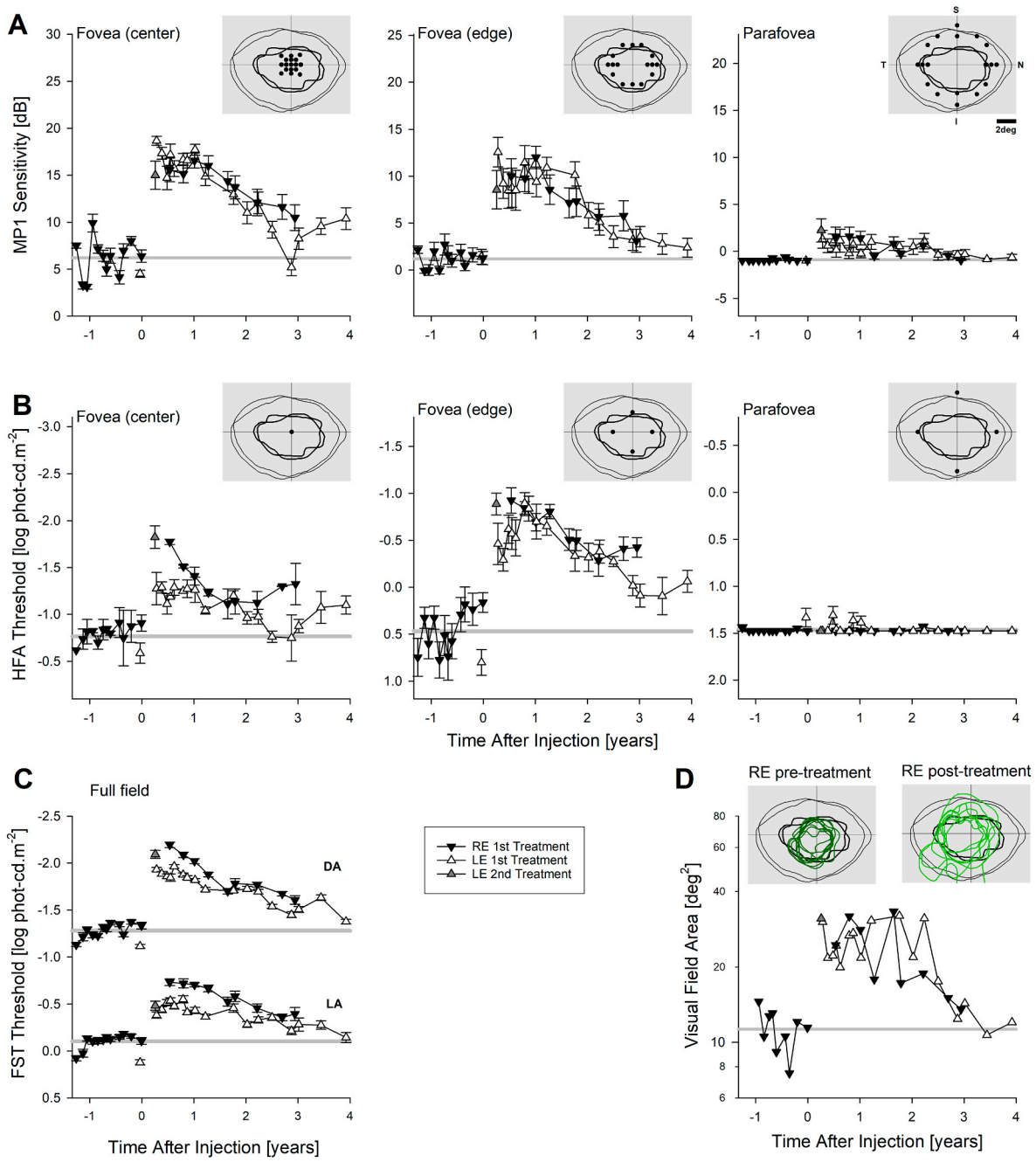

Fig. 3. Light sensitivity. **(A)** Retina-tracking microperimetry performed with white stimuli on a red background. **(B)** Dark-adapted chromatic perimetry performed with blue and red stimuli. Results from different test locations representing foveal center, foveal edge, and parafovea are segregated in panels A and B. Insets duplicate the baseline boundaries shown in Fig. 1 as a reference to the locations evaluated (black circles). **(C)** Dark-adapted (DA) and light-adapted (LA) FST thresholds. **(D)** Extent of visual field area estimated from retina-tracking microperimetry results shown in panel A. Insets show all visual field areas pre- and post-treatment in the RE overlaid to baseline boundaries shown in Fig. 1. Symbols in all panels comparable to Fig. 2. Error bars are ±SE. (For interpretation of the references to color in this figure legend, the reader is referred to the Web version of this article.)

log units followed by steady decline towards baseline between 3 and 4 years post-injection (Fig. 3C).

To better understand changes in the effective visual field, we used retina-tracking perimetry results to estimate the vision boundaries over time. In the left eye (without baseline measurements), visual field area fluctuated near ~25 deg^2 for the first 2.5 years after the injection, showing evidence of shrinking thereafter. In the right eye, visual field area during the pre-treatment period was ~11 deg^2. It expanded to ~30 deg^2 within the first year of injection and showing evidence of progressive shrinking towards baseline thereafter (Fig. 3D).

To allow for understanding the subjective perceptions experienced, careful records were made as the patient would spontaneously describe anecdotes about changes in vision or provide responses when periodically asked to compare vision between both eyes. These interactions occurred either during study visits or as phone calls made to remotely monitor for safety when in-person visits could not be made, such as during the pandemic. The right eye was the dominant eye at enrollment and left eye was chosen to be treated (Suppl. Fig. 1). By the end of the first month following first injection in the left eye, patient reported slight improvement in vision of the left eye making the two eyes similar. By two months, the left eye had become dominant and was described as having more clarity, a greater ability to perceive brightness and by three

months, increased speed of reading text. As of 15 months after first injection, left eye remained dominant and right eye received an injection (Fig. 4A). The right eye regained dominance by the third month after dosing of the right eye. The patient had noticed improvements in acuity by the second month, followed by improvements in visual field by the third month. One month following the second dose of the left eye, the left eye was reported as having slight improvement and that there was no dramatic difference between the two eyes. The left eye became dominant by the third month following the second dose of the left eye.

Functional vision using a novel method of mobility performance in dark-adapted eyes was measured to link visual function measurements with subjective perceptions (Fig. 4B). This type of mobility testing was done at the last three visits before and after re-injection of the left eye. At age 17.6 years (27 months after the last right eye injection and 41 months after the last left eye injection) mobility task thresholds were substantially elevated but showed asymmetry that was consistent with

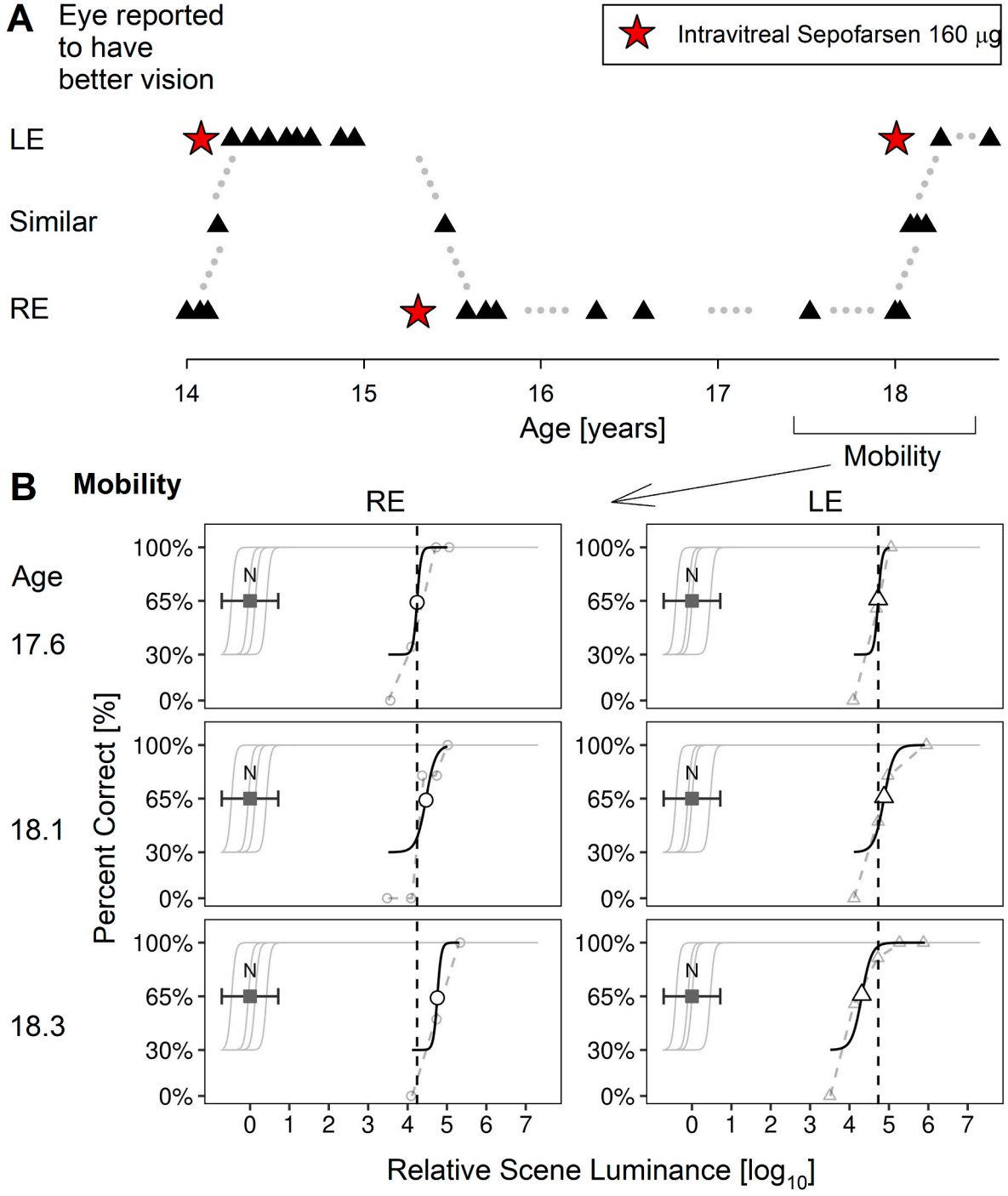

Fig. 4. Vision asymmetry perceived by patient and performance on mobility course. **(A)** Perception of the patient regarding eye with better vision (black triangles) during the 4.5 year period when sepofarsen injections were performed (red stars). **(B)** Thresholds for dark-adapted mobility estimated from sigmoid curves fit to success/failure data at different target luminances performed monocularly at three visits. Shifts to the left are improvements. Brackets: 95% confidence interval for threshold (circles) at each visit. N, normal population range; filled square, mean normal. Dashed gray lines joining small gray circles represent percent correct over 10 trials at each luminance. Dashed vertical black lines provide a reference to distinguish changes from the first visit. (For interpretation of the references to color in this figure legend, the reader is referred to the Web version of this article.)

the interval from last injection (4.2 and 4.7 l.u. from normal median for right and left eyes, respectively). Six months later, immediately before re-injecting the left eye, mobility thresholds had deteriorated by 0.2 l.u. in both eyes. Three months after the re-injecting left eye, the mobility task threshold of the left eye improved by 0.4 l.u. whereas the uninjected right eye threshold showed a further deterioration of 0.3 l.u.

To consider potential effects of progression of disease due to natural history or toxicity of sepofarsen, we evaluated RPE imaging results throughout the observation period. The extent of RPE melanization on NIRAF along horizontal and vertical major meridians did not show consistent changes (Figs. S1A–D). The intensity of the NIRAF near the fovea also did not show consistent changes (Fig. S1E) supporting a stable RPE disease in both eyes during the 4+ year observation period.

To evaluate subcellular scale changes to the photoreceptors, we quantified OCT layer thicknesses and backscatter intensities extending similar analyses previously performed for the first 15 months.[20] The thickness of the total retina showed no consistent changes at 4/5 sampled locations; at 1° nasal retina, there was a tendency for 10–20 μm thinning between 1 and 4 years after injection (Fig. S2). The thickness of the ONL showed no consistent changes at 3/5 sampled locations; at foveal center and 1° temporal retina, there was a tendency for 10–20 μm reduction (Fig. S3). IS thickness showed no consistent changes at 3/5 sampled locations; at foveal center and 1° temporal retina, there was a tendency for a transient 5–10 μm extension that returned to baseline by

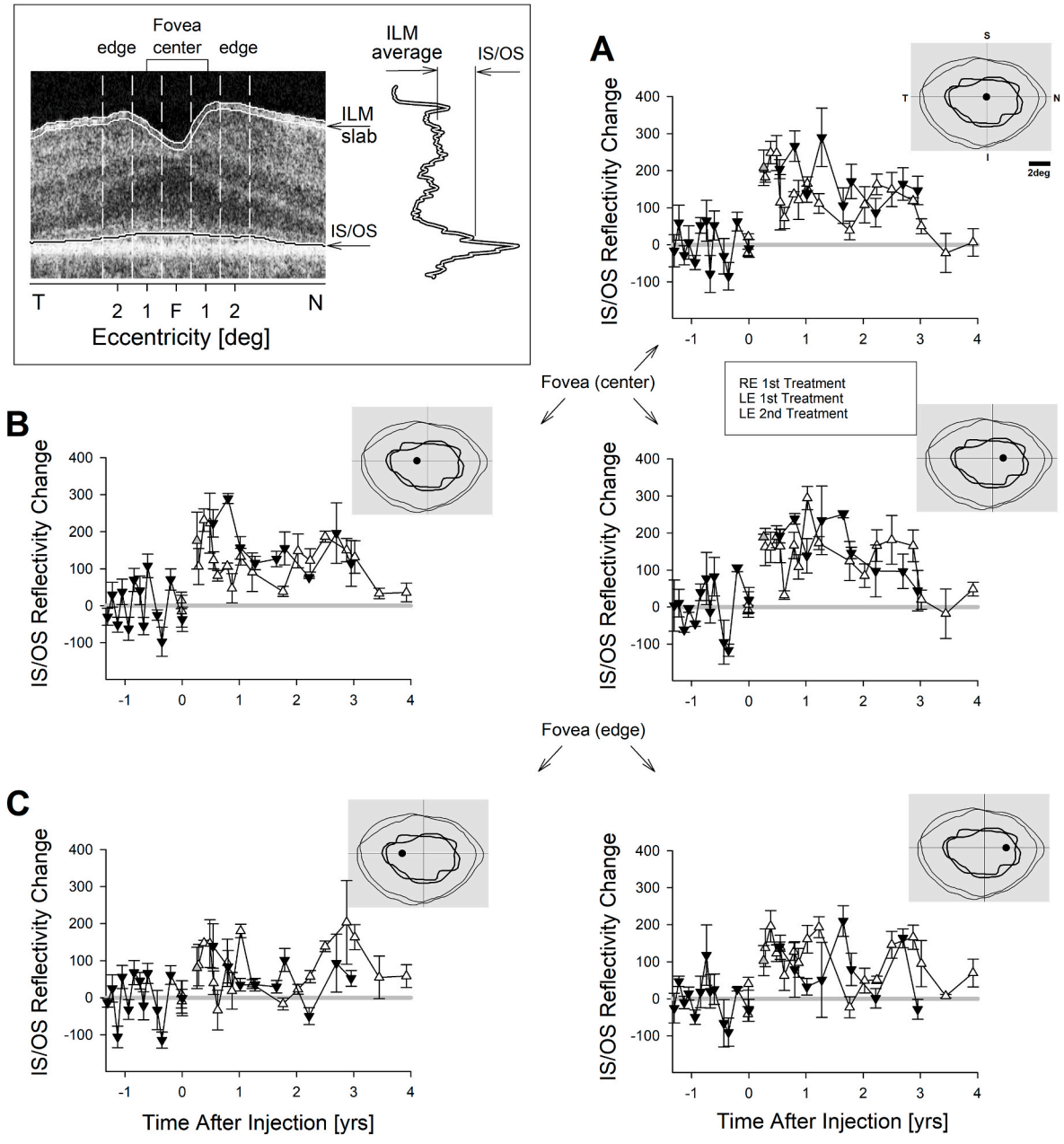

Fig. 5. Reflectivity at the IS/OS interface. **(Inset, upper left)** OCT scan at baseline showing three foveal center locations and two foveal edge locations sampled for the magnitude of the IS/OS peak intensity. Average ILM intensity is calculated from a 5 μm thick slab at the retina-vitreous interface and subtracted from IS/OS peak measurements to normalize visit to visit variation. The longitudinal reflectivity profile (LRP) on the right exemplifies the difference between IS/OS and average ILM intensities plotted. **(A,B,C)** Magnitude of the normalized IS/OS intensity as a function of time from each sepofarsen injection in each eye. Results from different test locations representing foveal center and foveal edge are segregated into different panels. Each symbol represents measurements from three independent scans. Insets in each panel duplicate the baseline boundaries of NIRAF extent and IS/OS extent shown in Fig. 1 as a reference to the locations evaluated (black circles). Symbols in all panels comparable to Figs. 2 and 3. Error bars are ±SE. Baseline values for each eye and each panel listed in Table S2.

3–4 years (Fig. S4). There were no changes to the outer segment length detectable (Fig. S5). Most relevant to the natural localization of CEP290 at the connecting cilium was the intensity of the IS/OS peak. Normalized IS/OS intensity at the three foveal center locations transiently increased after the injection and returned to baseline 3–4 years post-injection (Fig. 5A and B). At the foveal edge, data was more noisy and there were no obvious changes detectable (Fig. 5C).

4. Discussion

In common multifactorial diseases, evaluation of the human biological response to an investigational intervention must contend with substantial variability expected from genetic, stochastic, behavioral, and environmental factors interacting with age and individual difference of adherence to the drug regimen. Rare IRDs on the other hand, form the ideal basis for gene-based treatments where the response to a one-time intervention is expected to be more black-and-white. However, real-world biological response often is more complex than the ideal. For example, gene augmentation therapy in two distinct IRDs can produce light sensitivity improvements in the 4–5 $\log_{10}$ unit (10,000–100,000 fold) range in a matter of days; but, this indisputable positive outcome happens in some patients but not in others.[25,36–38] In the case of evaluating sepofarsen for *CEP290*-LCA, the population of patients is extremely homogeneous carrying the same exact allele in the same gene but previous results pointed to variation in response nevertheless.[19–22] In one eye of one hyper-responder subject P11, nearly a dozen outcome measures showed incontrovertible response that lasted at least 15 months.[20] Current work evaluated P11 (who carried the intronic variant homozygously) over a longer duration across multiple injections to both eyes to better understand and quantify the repeatability of the biological consequences of sepofarsen in human eyes.

We show the existence of a long tail of the foveal pharmacodynamics extending to 3–4 years following each single bolus injection. Pharmacodynamics as used in the current context is the temporal course of vision change measured at a specific retinal location as a function time from each intravitreal sepofarsen injection. Dominant contributors to the measured pharmacodynamics could include diffusion rates across the vitreous and retina, uptake rate across cellular and nuclear membranes, and clearance rate of sepofarsen. Upon successful masking of intron 26 in pre-mRNA by sepofarsen, rates of synthesis and degradation of CEP290 protein, rates of assembly and disassembly of multi-protein complexes involving CEP290 in the connecting cilium, and rates of cone opsin accumulation could be relevant. Also to be considered, is the rate of cellular loss or dysfunction due to natural history of *CEP290*-LCA or subclinical toxicity or inflammation caused by sepofarsen.

Multiple measures of visual function suggested a peak response being reached by 3 months after sepofarsen injections. Sepofarsen and other second generation AONs are thought to reach the retina and hybridize with pre-mRNA to perform therapeutic splicing in a time scale measured in minutes to hours.[18,39–41] So why does visual improvement take months to develop? CEP290 is a rod-like protein with coil-coiled structure[42,43] that may form multi-molecular complexes within the connecting cilium[44,45] involving possibly NPHP1, NPHP4, NPHP5, or NPHP8.[44–52] Rates of formation of such protein structures within the human foveal cone CC is not known but an extremely slow rate could potentially explain the delay of visual gains extending to weeks to months.

Durability of a transient physiological change resulting from an externally introduced biologic is expected to follow the degradation and clearance of the biologic from the cells/organ. The retinal half-life of second generation AONs including sepofarsen, has been estimated to be 2 months in non-human primate,[53] more than 1 month in mice,[54] and 2 months in rabbit.[18] The present study documented that vision improvement from a single injection of sepofarsen lasts 3–4 years suggesting a difference of more than an order of magnitude between the estimated pharmacokinetics of sepofarsen in the retina and pharmacodynamics of vision improvement. This large difference can be explained by hypothesizing that the natural turnover of CEP290 protein is exceedingly slow. We are not aware of measurements of CEP290 protein turnover in direct support of this conjecture. Indirectly however, it may be relevant that NPHP5, which is a binding partner CEP290, is thought to have low turnover in vitro.[55] Furthermore, both CEP290 as well as NPHP5 are thought to bind nucleoporins in primary cilia,[52] and some nucleoporins can have very slow turnover.[56]

5. Conclusion

Our current findings taken together with our previous results[19–22] support an indisputable improvement in foveal cone photoreceptor sensitivity resulting from 160 μg sepofarsen injection. The vision improvement is slow to rise to a peak and very slow to return to baseline, thus repeated injection regimens should not have intervals shorter than 2 years to reduce the risk of toxicity.

Author contributions

Conceptualization, A.V.C, S.G.J, A.C.H., M.R.S. and A.G.; methodology, A.V.C., M.S., A.S., A.J.R; formal analysis, A.V.C., M.S., A.S., A.J.R.; investigation, A.V.C., S.G.J., A.C.H., M.S., A.S., A.J.R., V.W., R.C.R., I.V.; writing—original draft preparation, A.V.C.; writing—review and editing, A.V.C., A.C.H., A.V.G.; supervision, A.V.C., S.G.J. and A.V.G.; funding acquisition, A.V.C. All authors have read and agreed to the published version of the manuscript.

Funding

This research was funded by ProQR Therapeutics, Leiden, The Netherlands and unrestricted funds from Research to Prevent Blindness.

Institutional review board statement

The study was conducted in accordance with the Declaration of Helsinki and approved by the Institutional Review Board of University of Pennsylvania (protocol codes 828007 for the initial study (initially approved August 30, 2017) and 831935 for the extension study (initially approved July 15, 2019)).

Patient consent

Consent to publish the case report was not obtained. This report does not contain any personal information that could lead to the identification of the patient.

Data availability statement

The data presented in this study are available on reasonable request from the corresponding author.

Declaration of competing interest

The authors declare the following financial interests/personal relationships which may be considered as potential competing interests. Michael R. Schwartz and Aniz Girach are employees of ProQR Therapeutics. All other authors have no known interests

Appendix A. Supplementary data

Supplementary data to this article can be found online at https://doi.org/10.1016/j.ajoc.2023.101873.

References

1. Bramall AN, Wright AF, Jacobson SG, McInnes RR. The genomic, biochemical, and cellular responses of the retina in inherited photoreceptor degenerations and prospects for the treatment of these disorders. *Annu Rev Neurosci*. 2010;33:441–472.
2. Verbakel SK, van Huet RAC, Boon CJF, et al. Non-syndromic retinitis pigmentosa. *Prog Retin Eye Res*. 2018;66:157–186.
3. Garafalo AV, Cideciyan AV, Héon E, et al. Progress in treating inherited retinal diseases: early subretinal gene therapy clinical trials and candidates for future initiatives. *Prog Retin Eye Res*. 2020;77:100827, 100827.
4. Kumaran N, Moore AT, Weleber RG, Michaelides M. Leber congenital amaurosis/early-onset severe retinal dystrophy: clinical features, molecular genetics and therapeutic interventions. *Br J Ophthalmol*. 2017;101(9):1147–1154.
5. den Hollander AI, Koenekoop RK, Yzer S, et al. Mutations in the CEP290 (NPHP6) gene are a frequent cause of Leber congenital amaurosis. *Am J Hum Genet*. 2006;79(3):556–561.
6. Perrault I, Delphin N, Hanein S, et al. Spectrum of NPHP6/CEP290 mutations in Leber congenital amaurosis and delineation of the associated phenotype. *Hum Mutat*. 2007;28(4):416.
7. Cideciyan AV, Aleman TS, Jacobson SG, et al. Centrosomal-ciliary gene CEP290/NPHP6 mutations result in blindness with unexpected sparing of photoreceptors and visual brain: implications for therapy of Leber congenital amaurosis. *Hum Mutat*. 2007;28(11):1074–1083.
8. Cideciyan AV, Rachel RA, Aleman TS, et al. Cone photoreceptors are the main targets for gene therapy of NPHP5 (IQCB1) or NPHP6 (CEP290) blindness: generation of an all-cone Nphp6 hypomorph mouse that mimics the human retinal ciliopathy. *Hum Mol Genet*. 2011;20(7):1411–1423.
9. Jacobson SG, Sumaroka A, Luo X, Cideciyan AV. Retinal optogenetic therapies: clinical criteria for candidacy. *Clin Genet*. 2013;84(2):175–182.
10. Jacobson SG, Cideciyan AV, Huang WC, et al. Leber congenital amaurosis: genotypes and retinal structure phenotypes. *Adv Exp Med Biol*. 2016;ume 854:169–175.
11. Jacobson SG, Cideciyan AV, Sumaroka A, et al. Outcome measures for clinical trials of leber congenital amaurosis caused by the intronic mutation in the CEP290 gene. *Invest Ophthalmol Vis Sci*. 2017;58(5):2609–2622.
12. Charng J, Jacobson SG, Heon E, et al. Pupillary light reflexes in severe photoreceptor blindness isolate the melanopic component of intrinsically photosensitive retinal ganglion cells. *Invest Ophthalmol Vis Sci*. 2017;58(7):3215–3224.
13. Cideciyan AV, Jacobson SG. Leber congenital amaurosis (LCA): potential for improvement of vision. *Invest Ophthalmol Vis Sci*. 2019;60(5):1680–1695.
14. Krishnan AK, Jacobson SG, Roman AJ, et al. Transient pupillary light reflex in CEP290- or NPHP5-associated Leber congenital amaurosis: latency as a potential outcome measure of cone function. *Vis Res*. 2020;168:53–63.
15. Sumaroka A, Garafalo AV, Semenov EP, et al. Treatment potential for macular cone vision in leber congenital amaurosis due to CEP290 or NPHP5 mutations: predictions from artificial intelligence. *Invest Ophthalmol Vis Sci*. 2019;60(7):2551–2562.
16. Collin RW, den Hollander AI, van der Velde-Visser SD, Bennicelli J, Bennett J, Cremers FP. Antisense oligonucleotide (AON)-based therapy for Leber congenital amaurosis caused by a frequent mutation in CEP290. *Mol Ther Nucleic Acids*. 2012;1:e14.
17. Gerard X, Perrault I, Hanein S, et al. AON-mediated exon skipping restores ciliation in fibroblasts harboring the common Leber congenital amaurosis CEP290 mutation. *Mol Ther Nucleic Acids*. 2012;1:e29.
18. Dulla K, Aguila M, Lane A, et al. Splice-modulating oligonucleotide QR-110 restores CEP290 mRNA and function in human c.2991+1655A>G LCA10 models. *Mol Ther Nucleic Acids*. 2018;12:730–740.
19. Cideciyan AV, Jacobson SG, Drack AV, et al. Effect of an intravitreal antisense oligonucleotide on vision in Leber congenital amaurosis due to a photoreceptor cilium defect. *Nat Med*. 2019;25(2):225–228.
20. Cideciyan AV, Jacobson SG, Ho AC, et al. Durable vision improvement after a single treatment with antisense oligonucleotide sepofarsen: a case report. *Nat Med*. 2021;27(5):785–789.
21. Cideciyan AV, Jacobson SG, Ho AC, et al. Restoration of cone sensitivity to individuals with congenital photoreceptor blindness within the phase 1/2 sepofarsen trial. *Ophthalmol Sci*. 2022;2, 100133.
22. Russell SR, Drack AV, Cideciyan AV, et al. Intravitreal antisense oligonucleotide sepofarsen in Leber congenital amaurosis type 10: a phase 1b/2 trial. *Nat Med*. 2022;28(5):1014–1021.
23. Ferris 3rd FL, Kassoff A, Bresnick GH, Bailey I. New visual acuity charts for clinical research. *Am J Ophthalmol*. 1982;94(1):91–96.
24. Sunness JS, Rubin GS, Broman A, Applegate CA, Bressler NM, Hawkins BS. Low luminance visual dysfunction as a predictor of subsequent visual acuity loss from geographic atrophy in age-related macular degeneration. *Ophthalmology*. 2008;115(9):1480–1488.
25. Jacobson SG, Cideciyan AV, Ho AC, et al. Night vision restored in days after decades of congenital blindness. *iScience*. 2022;25(10), 105274.
26. Roman AJ, Schwartz SB, Aleman TS, et al. Quantifying rod photoreceptor-mediated vision in retinal degenerations: dark-adapted thresholds as outcome measures. *Exp Eye Res*. 2005;80(2):259–272.
27. Roman AJ, Cideciyan AV, Aleman TS, Jacobson SG. Full-field stimulus testing (FST) to quantify visual perception in severely blind candidates for treatment trials. *Physiol Meas*. 2007;28(8):N51–N56.
28. Roman AJ, Cideciyan AV, Wu V, Garafalo AV, Jacobson SG. Full-field stimulus testing: role in the clinic and as an outcome measure in clinical trials of severe childhood retinal disease. *Prog Retin Eye Res*. 2022;87, 101000.
29. Cideciyan AV, Krishnan AK, Roman AJ, Sumaroka A, Swider M, Jacobson SG. Measures of function and structure to determine phenotypic features, natural history, and treatment outcomes in inherited retinal diseases. *Annu Rev Vis Sci*. 2021;7(1).
30. Roman AJ, Cideciyan AV, Wu V, et al. Mobility test to assess functional vision in dark-adapted patients with Leber congenital amaurosis. *BMC Ophthalmol*. 2022;22(1):266.
31. Cideciyan AV, Swider M, Aleman TS, et al. Reduced-illuminance autofluorescence imaging in ABCA4-associated retinal degenerations. *J Opt Soc Am A*. 2007;24(5):1457, 1457.
32. Cideciyan AV, Hufnagel RB, Carroll J, et al. Human cone visual pigment deletions spare sufficient photoreceptors to warrant gene therapy. *Hum Gene Ther*. 2013;24(12):993–1006.
33. Shlaer S, Smith EL, Chase AM. Visual acuity and illumination in different spectral regions. *J Gen Physiol*. 1942;25(4):553–569.
34. Wood LJ, Jolly JK, Buckley TM, Josan AS, MacLaren RE. Low luminance visual acuity as a clinical measure and clinical trial outcome measure: a scoping review. *Ophthalmic Physiol Opt*. 2021;41(2):213–223.
35. Hess K, Gliem M, Birtel J, et al. Impaired dark adaptation associated with a diseased bruch membrane in pseudoxanthoma elasticum. *Retina*. 2020;40(10):1988–1995.
36. Cideciyan AV, Aleman TS, Boye SL, et al. Human gene therapy for RPE65 isomerase deficiency activates the retinoid cycle of vision but with slow rod kinetics. *Proc Natl Acad Sci USA*. 2008;105(39):15112–15117.
37. Jacobson SG, Cideciyan AV, Ratnakaram R, et al. Gene therapy for leber congenital amaurosis caused by RPE65 mutations: safety and efficacy in 15 children and adults followed up to 3 years. *Arch Ophthalmol*. 2012;130(1):9–24.
38. Jacobson SG, Cideciyan AV, Ho AC, et al. Safety and improved efficacy signals following gene therapy in childhood blindness caused by GUCY2D mutations. *iScience*. 2021;24(5):102409, 102409.
39. Juliano RL, Ming X, Carver K, Laing B. Cellular uptake and intracellular trafficking of oligonucleotides: implications for oligonucleotide pharmacology. *Nucleic Acid Therapeut*. 2014;24(2):101–113.
40. Murray SF, Jazayeri A, Matthes MT, et al. Allele-specific inhibition of rhodopsin with an antisense oligonucleotide slows photoreceptor cell degeneration. *Invest Ophthalmol Vis Sci*. 2015;56(11):6362–6375.
41. Dulla K, Slijkerman R, van Diepen HC, et al. Antisense oligonucleotide-based treatment of retinitis pigmentosa caused by USH2A exon 13 mutations. *Mol Ther*. 2021;29(8):2441–2455.
42. Rachel RA, Yamamoto EA, Dewanjee MK, et al. CEP290 alleles in mice disrupt tissue-specific cilia biogenesis and recapitulate features of syndromic ciliopathies. *Hum Mol Genet*. 2015;24(13):3775–3791.
43. Mookherjee S, Chen HY, Isgrig K, et al. A CEP290 C-terminal domain complements the mutant CEP290 of rd16 mice in trans and rescues retinal degeneration. *Cell Rep*. 2018;25(3):611–623 e616.
44. Wensel TG, Potter VL, Moye A, Zhang Z, Robichaux MA. Structure and dynamics of photoreceptor sensory cilia. *Pflügers Archiv*. 2021;473(9):1517–1537.
45. Potter VL, Moye AR, Robichaux MA, Wensel TG. Super-resolution microscopy reveals photoreceptor-specific subciliary location and function of ciliopathy-associated protein CEP290. *JCI Insight*. 2021;6(20), e145256.
46. Schafer T, Putz M, Lienkamp S, et al. Genetic and physical interaction between the NPHP5 and NPHP6 gene products. *Hum Mol Genet*. 2008;17(23):3655–3662.
47. Sang L, Miller JJ, Corbit KC, et al. Mapping the NPHP-JBTS-MKS protein network reveals ciliopathy disease genes and pathways. *Cell*. 2011;145(4):513–528.
48. Shiba D, Yokoyama T. The ciliary transitional zone and nephrocystins. *Differentiation*. 2012;83(2):S91–S96.
49. Barbelanne M, Song J, Ahmadzai M, Tsang WY. Pathogenic NPHP5 mutations impair protein interaction with Cep290, a prerequisite for ciliogenesis. *Hum Mol Genet*. 2013;22(12):2482–2494.
50. Barbelanne M, Hossain D, Chan DP, Peranen J, Tsang WY. Nephrocystin proteins NPHP5 and Cep290 regulate BBSome integrity, ciliary trafficking and cargo delivery. *Hum Mol Genet*. 2015;24(8):2185–2200.
51. Takao D, Wang L, Boss A, Verhey KJ. Protein interaction analysis provides a map of the spatial and temporal organization of the ciliary gating zone. *Curr Biol*. 2017;27(15):2296–2306 e2293.
52. Blasius TL, Takao D, Verhey KJ. NPHP proteins are binding partners of nucleoporins at the base of the primary cilium. *PLoS One*. 2019;14(9), e0222924.
53. Henry SP, Miner RC, Drew WL, et al. Antiviral activity and ocular kinetics of antisense oligonucleotides designed to inhibit CMV replication. *Invest Ophthalmol Vis Sci*. 2001;42(11):2646–2651.
54. Gérard X, Perrault I, Munnich A, Kaplan J, Rozet JM. Intravitreal injection of splice-switching oligonucleotides to manipulate splicing in retinal cells. *Mol Ther Nucleic Acids*. 2015;4(9), e250.
55. Das A, Qian J, Tsang WY. USP9X counteracts differential ubiquitination of NPHP5 by MARCH7 and BBS11 to regulate ciliogenesis. *PLoS Genet*. 2017;13(5), e1006791.
56. Savas JN, Toyama BH, Xu T, Yates 3rd JR, Hetzer MW. Extremely long-lived nuclear pore proteins in the rat brain. *Science*. 2012;335(6071):942.